Rotational spectra and structure of the ammonia–water complex

Cite as: J. Chem. Phys. **83**, 3768 (1985); https://doi.org/10.1063/1.449139
Submitted: 01 February 1985 . Accepted: 12 June 1985 . Published Online: 31 August 1998

P. Herbine, and T. R. Dyke

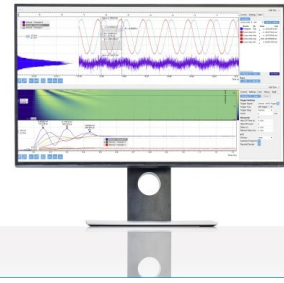

Rotational spectra and structure of the ammonia–water complex

P. Herbine and T. R. Dyke
Department of Chemistry, University of Oregon, Eugene, Oregon 97403

(Received 1 February 1985; accepted 12 June 1985)

Microwave and radio frequency spectra for $NH_3 \cdot H_2O$ and deuterated analogs have been observed by molecular beam electric resonance spectroscopy. Rotational constant, Stark effect, and nitrogen quadrupole coupling interaction data were obtained. This complex is found to have a linear, hydrogen bonded structure with water as the proton donor. The NH_3 monomer symmetry axis was found to have a vibrationally averaged displacement of 23.1° from the N...O axis. No evidence for transfer of a proton from water to the ammonia was observed.

INTRODUCTION

Among the earliest recognitions that hydrogen bonds existed and represented unique bonding situations were papers by Werner[1] and by Moore and Winmill[2] concerning substituted ammonium compounds such as "R_3N–H–OH." We have observed microwave and radio frequency spectra for one of the simplest of these compounds $NH_3 \cdot H_2O$ using the molecular beam electric resonance method.

Hydrogen bonds of this type appear in a variety of more complicated systems including aqueous solutions and crystalline solids. N...H–O hydrogen bonds are formed in biologically important macromolecules and complexes involving H_2O are ubiquitous. Recently[3–5] detailed structural studies of several ammonia containing complexes have been reported. It is hoped this work will shed light on the details of hydrogen bonding and help in understanding the more complicated systems mentioned above.

EXPERIMENTAL

Microwave and radio frequency spectra for ammonia–water complexes were obtained by the molecular beam electric resonance method, which is discussed in detail elsewhere.[6] The pertinent features of our apparatus[7] are linewidths of typically 3 kHz for radio frequency transitions and somewhat broader widths of 20 kHz, caused by Doppler effects, for microwave transitions. For $NH_3 \cdot H_2O$ and deuterated analogs, substantially broader lines were observed ($\sim$100 kHz) as shown in Fig. 1, from the overlapping of large numbers of lines split by small hydrogen and deuterium nuclear spin interactions. Frequencies were counted to accuracies of better than $1{:}10^7$ and thus molecular transition frequencies were limited in accuracy by the width of the unresolved hyperfine components. Stark effect measurements were made by varying the electric field strength in the resonance region. These field strengths were determined by calibration with an OCS standard.[8] Electric dipole moment measurements accurate to better than $2{:}10^4$ were achieved by these methods.

Molecular beams of $NH_3 \cdot H_2O$ were generated by expanding a mixture of 2% H_2O and 3% NH_3 in 1000 Torr of argon through a 25 μ diameter nozzle source. The gas mixtures were conveniently made by bubbling the ammonia and argon through an approximately 2 M NH_3, aqueous solutions at 25 °C. Relatively pure $ND_3 \cdot D_2O$ was prepared by first synthesizing ND_3 from CaN_2 and D_2O, and then bubbling ND_3–argon mixture through D_2O as above. For partial deuteration, NH_3–argon mixtures were bubbled through D_2O/H_2O solutions with the desired mole fraction of deuterium.

The molecular beams were detected with an electron impact ionizer, mass spectrometer. The strongest signals for $NH_3 \cdot H_2O$ were observed with this detector set at mass 18 and for $ND_3 \cdot D_2O$ at mass 22. The ions detected were presumably NH_4^+ and ND_4^+, although H_2O^+ could be a contributor to the $NH_3 \cdot H_2O$ signal. The ambiguity was not resolved by observing the ratio of $ND_3 \cdot D_2O$ signals at mass 22 (ND_4^+) and mass 20 (D_2O^+, ND_3^+) because an Ar^{2+} ion dominated the intensity at mass 20. The partially deuterated complexes cannot be solely identified by the mass spectral features used to detect a set of transitions. However, a third species in addition to $NH_3 \cdot H_2O$ and $ND_3 \cdot D_2O$ was identified as $NH_3 \cdot DOH$ by its small shift in frequencies from the $NH_3 \cdot H_2O$ rotational transitions, i.e., the deuterium is very close to the center-of-mass for this species and only slightly lowers the rotational constants. A fourth species was observed which, from its spectrum and the structure discussed later on, must be either $NH_2D \cdot H_2O$ or $NH_3 \cdot HOD$. Consideration of the various exchange equilibria

$$NH_3 + HOD \rightleftarrows NH_2D + H_2O, \quad (1a)$$

$$NH_2D + HOD \rightleftarrows NHD_2 + H_2O, \text{ etc.}, \quad (1b)$$

predicts a 3:2 excess of HOD over NH_2D in the nozzle source before the expansion, slightly favoring $NH_3 \cdot HOD$ as the species observed. In addition, the signals are observed more strongly at mass 18 than at mass 19, which could be explained by assuming that NX_4^+ (x = H or D) is the pre-

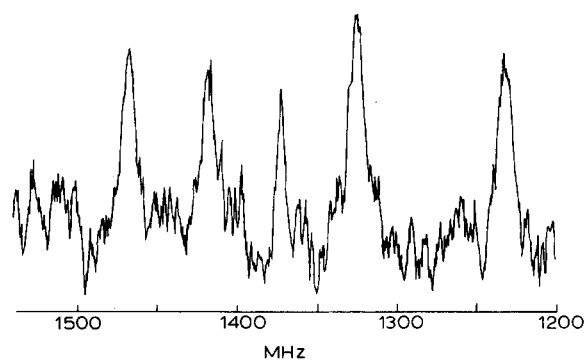

FIG. 1. Hyperfine splittings of the $J = 1, M = 0 - 1$ transition of ammonia water. The Stark field is 499.600 V/cm.

 0021-9606/85/203768-07$02.10

dominant fragment ion, and that the hydrogen-bonded hydrogen is selectively donated in the fragmentation process

$$NH_3{\cdot}D|OH \xrightarrow{e^-} NH_3D^+ + OH^-. \quad (2)$$

This argument is rather speculative, and although there is some evidence favoring $NH_3{\cdot}HOD$ over $NH_2D{\cdot}H_2O$ for this fourth species, this assignment remains ambiguous.

RESULTS

Radio frequency and microwave spectra for $K=0$ states of $NH_3{\cdot}H_2O$ and deuterated analogs were observed at several electric field strengths in the resonance region, and the resulting frequencies are given in Tables I and II. The A rotational constant of $NH_3{\cdot}H_2O$ is predicted to be 5 cm^{-1}, and thus $K>0$ states have substantially lower populations than $K=0$ states in the low temperature argon expansions. Although a moderately strong continuum of transitions was observed at zero electric field from K-doubling transitions, resolved spectra for states with $K>0$ were not observed because of the low populations of these states.

For $NH_3{\cdot}H_2O$, $J,|M_J|=1,0\rightarrow1,1$ and $2,1\rightarrow2,2$ radio frequency transitions were observed as were the $1,0\rightarrow0,0$ and $2,0\rightarrow1,1$ microwave transitions. For $ND_3{\cdot}D_2O$, the $1,0\rightarrow1,1$ and $1,0\rightarrow0,0$ transitions were measured, and for the partially deuterated species, only the $1,0\rightarrow0,0$ microwave transitions were studied. Less data for the deuterated species were taken because of lower signal-to-noise ratios. As shown in Fig. 1, the spectra consist of broad (100 kHz) clumps of lines separated by several hundred kilohertz. This large

TABLE I. Radio frequency and microwave transitions for $NH_3{\cdot}H_2O$. Residuals ($\nu_{exp}-\nu_{calc}$) from the least squares procedure mentioned in the text are given in parentheses for each frequency.

	$NH_3{\cdot}H_2O$					
Electric field (V/cm)	Frequencies, $J=1$, $M_J=0\rightarrow1$ ($M_F\rightarrow M'_F$) (kHz)					
	(1→0)	(1→2)	(0→0)	(1→1)	(1→0)	(0→1)
249.79	2220(+ 9)	3020(− .4)	3250(+ 37)	3560(+ 7)	3970(+ 12)	...
299.75	3660(+ 2)	4520(+ 13)	4690(+ 49)	5020(− 1)	...	...
349.70	5440(+ 37)	6270(− 5)	...	...	...	...
399.66	7460(+ 27)	8330(+ 9)	...	8840(+ 25)	9280(+ 21)	9790(− 12)
499.58	12320(− 11)	13250(+ 13)	...	13720(− 2)	14180(+ 5)	14680(+ 4)
599.49	18240(− 90)	19240(− 6)	...	19750(+ 24)	20200(+ 16)	20620(− 55)
649.45	21730(− 10)	22670(+ 10)	...	23140(+ 2)	23600(+ 3)	24100(+ 15)

	$J=2$, $M_J=1\rightarrow2$ (kHz)	
	(0→1)	(1→2)
599.49	5120(+ 12)	5480(+ 7)
799.32	8763(+ 10)	9100(− 8)
1053.10	14900(− 6)	15241(− 14)
1198.98	19210(+ 1)	19560(+ 4)
1498.73	29798(+ 3)	30140(− .2)

	$J,M_J=1,0\rightarrow0,0$ (MHz)			
	(1→1)		(0→0)	
349.70	12296.786	(− .002)	...	
399.66	12300.432	(+ .007)	...	
449.62	12304.537	(− .012)	...	
499.58	12309.174	(+ .016)	12310.132	(+ .000)
549.53	12314.246	(− .006)	...	
599.49	12319.821	(− .008)	...	
649.45	12325.889	(+ .001)	...	
699.41	12332.433	(+ .005)	...	
749.36	12339.452	(+ .004)	...	
799.32	12346.944	(− .004)	...	

	$J,M_J=2,0\rightarrow1,1$ (MHz)			
	(1→0)		(1→2)	
849.28	24587.722	(− .010)	24588.602	(− .017)
1198.98	24607.077	(+ .005)	24607.994	(+ .009)
1498.73	24628.928	(− .015)	24629.866	(+ .008)

TABLE II. Radio frequency and microwave transitions for deuterated ammonia–water species. Residuals ($\nu_{exp} - \nu_{calc}$) are given in parentheses.

Field (V/cm)	Frequency (kHz) (1→0)	(1→2)
	$ND_3{\cdot}D_2O$ $J=1,\ M_J=0\rightarrow1\ (M_F\rightarrow M_F')$	
449.62	11 960 (−21)	12 950 (−3)
499.58	15 130 (+14)	16 090 (+1)
549.53	18 610 (+27)	19 560 (−1)
599.49	22 360 (−20)	23 360 (−2)
	$J,M_J,M_F = 1,0,1\rightarrow0,0,1$ (MHz)	
524.55	10 420.539 (+1)	
549.53	10 423.690 (−1)	
599.49	10 430.429 (+1)	
	$NH_3{\cdot}DOH$ $J,M_J,M_F = 1,0,1\rightarrow0,0,1$ (MHz)	
449.62	12 291.831	
499.58	12 296.510	
	$NH_3{\cdot}HOD$ or $NH_2D{\cdot}H_2O$ $J,M_J,M_F = 1,0,1\rightarrow0,0,1$ (MHz)	
349.70	11 772.119 (−1)	
399.66	11 775.962 (+2)	
449.62	11 780.311 (−2)	
499.58	11 785.179 (+1)	

spacing is caused by the nitrogen quadrupole coupling interaction[9]:

$$H_{hfs} = \frac{-\langle eqQ\rangle_{aa}}{2I(2I-1)(2J+3)(2J-1)} \times [3(\mathbf{I}\cdot\mathbf{J})^2 + 3/2\mathbf{I}\cdot\mathbf{J} - (\mathbf{I}\cdot\mathbf{I})(\mathbf{J}\cdot\mathbf{J})]. \quad (3)$$

In addition, $NH_3{\cdot}H_2O$ has 32 hydrogen spin states and a correspondingly larger number for the deuterated species. Internal rotation and NH_3 inversion are probably occurring at substantial rates, reducing the number of spin species compatible with a particular tunneling rotational state. Nonetheless, the number of hyperfine components caused by the hydrogen nuclear spins will be large and the splittings small (100 kHz), leading to the 100 kHz wide lines and precluding resolving them into component lines.

The microwave transitions were analyzed with the energy level expression for $K = 0$:

$$W_R = \frac{B+C}{2} J(J+1) - D_J J^2(J+1)^2. \quad (4)$$

In addition, the Stark effects for the microwave and radio frequency spectra are accounted for with the following:

$$W_s = \frac{\mu^2 E^2 J(J+1) - 3M_J^2}{(B+C)J(J+1)(2J+3)(2J-1)} + C_4 E^4, \quad (5)$$

where the fourth-order Stark term is a small correction, 100 kHz or less, at the electric fields used. Each microwave and radio frequency transition $JM_J \rightarrow J'M_J'$ consisting of one or more hyperfine components tracked as a function of electric field, were used in a least-square fitting procedure using Eqs. (3)–(5) to generate energy level and transition frequency expressions. For the $NH_3{\cdot}H_2O$ transitions, enough data was available to obtain a zero-field frequency (for the microwave lines), an electric dipole moment, and $\langle eqQ\rangle_{aa}$ for each transition. This was also done for the $ND_3{\cdot}D_2O$ $J,\ M_J = 1,0\rightarrow1,1$ transition. For the remaining microwave lines, only the most intense hyperfine component was tracked as a function of electric field, and thus the hyperfine splitting was calculated by transferring the appropriate $\langle eqQ\rangle_{aa}$ from $NH_3{\cdot}H_2O$ or $ND_3{\cdot}D_2O$. The residuals from this fitting procedure are also given in Tables I and II and the constants are reported in Tables III–V along with their standard deviations. Finally, the zero-field microwave frequencies were used to obtain $(B+C)/2$ and D_J for $NH_3{\cdot}H_2O$. For the remaining species, the small D_J term was calculated from the $NH_3{\cdot}H_2O$ result with the approximate expression

$$D_J \propto 1/\mu_r^2, \quad (6)$$

where μ_r is the psuedodiatomic reduced mass of the complex. The approximate value of D_J from Eq. (6) along with the zero-field microwave frequencies allowed $(B+C)/2$ to be calculated (Table V).

The electric dipole moments are displayed inTable III. The variations in the effective moments calculated for different transitions suggest that a small correction to Eq. (5) should be made due to b- and c-dipole moment components. Their effect is minor, because the A-rotational constant is large, and to an adequate approximation, the effective mo-

TABLE III. Electric dipole moments (in Debyes). An effective dipole moment is calculated from the Stark effect for each transition. For $NH_3{\cdot}H_2O$ and $ND_3{\cdot}D_2O$, μ_a and $\mu_\perp$ can be calculated from the effective moments. Standard deviations are given in parentheses.

Transition ($JM_J\rightarrow J'M_J'$)	μ_{eff} (exp)	[a] μ_{eff} (calc)	
	$NH_3{\cdot}H_2O$		
10→11	2.9788(5)	2.9790	
21→22	2.9850(4)	2.9839	$\mu_a = 2.9766(8)$
10→00	2.9768(3)	2.9775	[b] $\mu_\perp = 0.52(5)$
20→11	2.9814(6)	2.9806	
	$ND_3{\cdot}D_2O$		
10→11	3.0149(10)	...	$\mu_a = 2.9928(24)$
10→00	3.0011(15)	...	[c] $\mu_\perp = 1.21(8)$
	$NH_3{\cdot}DOH$		
10→00	2.992(3)	...	
	$NH_2D{\cdot}H_2O$ or $NH_3{\cdot}HOD$		
10→00	2.998(3)	...	

[a] Calculated from μ_a and $\mu_\perp$ with Eq. (7).
[b] Calculated with $A = 153$ GHz. The error given does not include the roughly 10% uncertainty in A.
[c] $A = 76$ GHz ($\pm$ 10%).

TABLE IV. Quadrupole constants for $NH_3 \cdot H_2O$ and $ND_3 \cdot D_2O$.

Transition $J,M_J \rightarrow J',M'_J$	$\langle eqQ \rangle_{aa}$ (MHz)
	$NH_3 \cdot H_2O$
1,0→1,1	−3.126 (19)
2,1→2,2	−3.182 (30)
1,0→0,0	−3.190 (31)
2,0→1,1	−3.060 (44)
Weighted average	−3.143 (14)
	$ND_3 \cdot D_2O$
1,0→1,1	−3.344 (38)

ments in Table III can be expressed as[10]

$$J,M_J = 1,0 \rightarrow 1,1 \quad \mu_a^2 + \frac{2}{3}\frac{B+C}{A}\mu_\perp^2,$$

$$2,1 \rightarrow 2,2 \quad \mu_a^2 + 2\frac{B+C}{A}\mu_\perp^2,$$

$$1,0 \rightarrow 0,0 \quad \mu_a^2 + \frac{1}{4}\frac{B+C}{A}\mu_\perp^2,$$

$$2,0 \rightarrow 1,1 \quad \mu_a^2 + \frac{24}{31}\frac{B+C}{A}\mu_\perp^2, \tag{7}$$

where $\mu_\perp = [\mu_b^2 + \mu_c^2]^{1/2}$. The resulting μ_a and $\mu_\perp$ values are also given in Table III. It should be noted that the A-rotational constant is predicted from the structure discussed below, but is not experimentally measured. This adds an additional uncertainty of roughly 10% in the $\mu_\perp$ results. Despite these uncertainties, a large increase in $\mu_\perp$ upon deuteration is clearly evident, and as discussed later, is presumably caused by a large amplitude oscillations of the monomers relative to one another, which are strongly reduced with increased reduced mass. The reduction can increase $\mu_\perp$ both by increasing the average projection of μ along the b axis (or c axis) and by reducing tunneling splittings which would be expected to increase the apparent A-rotational constant in Eq. (7) by increasing the $K = 0$ to 1 energy separation.

STRUCTURAL ANALYSIS

The rotational constants listed in Table V and the $\langle eqQ \rangle_{aa}$ data in Table IV contain information concerning the distance between the constituent monomers of the complex and their relative orientations. The coordinate system used to describe the complex is shown in Fig. 2. The distance between the monomers is specified by the O···N distance R which is independent of the isotopic species. In addition, it will be useful to use a closely related coordinate, the distance between the centers-of-mass of the monomers, denoted $R_{c.m.}$, which is isotopic species dependent. The orientations of the monomers are conveniently described by the Euler angles[11] ϕ,θ,χ with a subscript O or N to denote H_2O or NH_3. One of the angles ϕ can be arbitrarily fixed at zero and we have chosen $\phi_O = 0$.

The orientation of the ammonia group can be calculated from the nitrogen quadrupole coupling constants in Table IV by assuming the field gradient near the nitrogen nucleus to be the same in the complex as in free ammonia. The measured coupling constants are then the vibrationally averaged projection of the NH_3 quadrupole coupling tensor along the a axis (nearly the O···N axis) of the complex:

$$\langle eqQ \rangle_{aa} = eqQ^\circ \langle 3/2 \cos^2\theta_N - 1/2 \rangle, \tag{8}$$

where eqQ° is the free NH_3 value of −4.089 65 MHz.[12] The result is an effective angle, $\theta'_N = 23.1(2)^\circ$ for $NH_3 \cdot H_2O$ and $\theta'_N = 20.4\ (5)^\circ$ for $ND_3 \cdot D_2O$, where

$$\theta'_N = \cos^{-1}[\langle \cos^2\theta_N \rangle]^{1/2}. \tag{9}$$

These angles are very similar to the analogous angular displacements observed in other NH_3 complexes,[3–5] from symmetry axes assumed for their equilibrium geometries. If the inertia tensor is symmetric, or approximately so, in some displacement from the equilibrium structure, the observed rotational constants will be more characteristic of the root-mean-square vibrational deviation from equilibrium than of the equilibrium structure itself. This is the situation which would hold for $NH_3 \cdot H_2O$ if $\theta_N = 0^\circ$ at equilibrium with a 23° root-mean-square NH_3 amplitude. A similar interpretation is assumed for the complexes alluded to above.[3–5] This picture is further supported in our experiments by the decrease in θ'_N upon deuteration. In a harmonic oscillator model, the root-mean-square amplitude should decrease by roughly $2^{1/4}$ for the deuterated ammonia complex, resulting in a 5° change. The observed decrease is about half of that, and an equilibrium angle of 12° with a 20° vibrational amplitude better fits the data. Because of anharmonicity and possible

TABLE V. $(B+C)/2$ and D_J for $NH_3 \cdot H_2O$ and other isotopically substituted species.

Molecule	$(B+C)/2$ (MHz)	D_J (MHz)
$NH_3 \cdot H_2O$	6142.652 (3)	0.0367 (10)
$NH_3 \cdot DOH$	6136.14 (10)	(0.035)[a]
$NH_3 \cdot HOD$ or $NH_2D \cdot H_2O$	5879.99 (2)	(0.035)[a]
$ND_3 \cdot D_2O$	5194.288 (9)	(0.028)[a]

[a] Scaled from D_J for $NH_3 \cdot H_2O$ with Eq. (6) and used to calculate $(B+C)/2$ from the $J = 1 \rightarrow 0$ microwave transition.

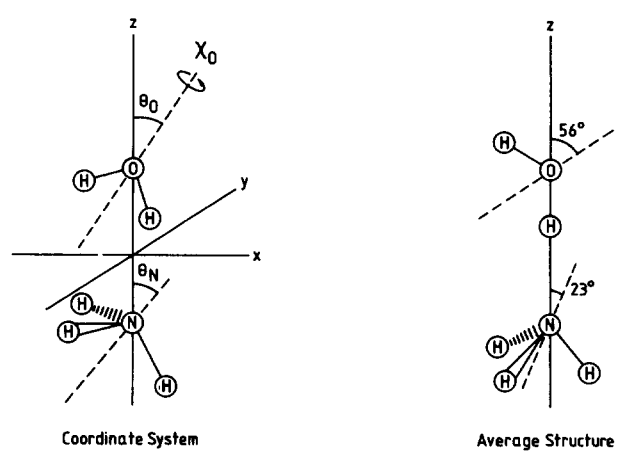

FIG. 2. Euler angles and final structure as described in the text.

changes in the NH_3 field gradient in the hydrogen bonded complex, this calculation is not accurate, but does indicate that the interpretation of θ'_N as a root-mean-square displacement from an equilibrium position near the N···O axis is reasonable.

Further information about the distance between the monomers and their orientations can be found from the $(B+C)/2$ data in Table V. These rotational constants are primarily sensitive to the O···N separation R and are less dependent on the Euler angles. The isotopic species which were unambiguously assigned were $NH_3{\cdot}H_2O$, $NH_3{\cdot}D_2O$, and $NH_3{\cdot}DOH$. The $(B+C)/2$ constants for these species are primarily dependent upon the angles θ_N, θ_O, and, to a lesser extent χ_O. This is easily seen from an approximate expression[13] for $(B+C)/2$:

$$(B+C)/2 \simeq B_0\Big\{1-\frac{1}{2I_0}[(i^0_{yy}+i^0_{zz}\sin^2\theta_O\cos^2\chi_O + i^0_{xx}\cos^2\theta_O + i^0_{xz}\sin 2\theta_O\cos\chi_O)_{H_2O} + (i^0_{xx}+i^0_{xx}\cos^2\theta_N + i^0_{zz}\sin^2\theta_N)_{NH_3}] + \cdots\Big\}, \tag{10}$$

$$B_0=\frac{\hbar^2}{2I_0}=\frac{\hbar^2}{2\mu R^2_{cm}}; \quad \mu=\frac{m_{H_2O}m_{NH_3}}{m_{H_2O}+m_{NH_3}}. \tag{11}$$

$i^\circ_{\alpha\beta}$ in Eq. (10) is the appropriate monomer moment of inertia and I_O is the psuedodiatomic moment of inertia of the complex. The largest terms omitted from Eq.(10) are of order of $(i^\circ_{\alpha\beta}/I_O)^2$, and thus represent an error of about 0.1% or 10 MHz in $(B+C)/2$. The angle dependent terms in Eq. (10) large enough to be useful are several percent of the dominant pseudodiatomic term B_O and thus the angles θ_O, θ_N, and χ_O can be determined from this data. ϕ_N occurs only in the higher-order terms omitted from Eq. (10). Since the magnitude of these terms is comparable to zero-point vibrational effects not considered in this model, ϕ_N is not determined. In addition, since a rotation around the NH_3 or ND_3 symmetry axis leaves the inertia tensor invariant, the rotational constants for complexes containing these species are independent of χ_N.

The coordinates which can then be calculated from the rotational constants are R, θ_O, θ_N, and χ_O. Since only three $(B+C)/2$ values were unambiguously assigned θ_N, or more precisely $\cos^2\theta_N$, was fixed at the value given by the quadrupole coupling results. The rotational constants depend on θ_N through $\cos^2\theta_N$ (and $\sin^2\theta_N = 1-\cos^2\theta_N$) as does $\langle eqQ\rangle_{aa}$, which is shown by Eqs. (8) and (10). R, θ_O, and χ_O were then varied to fit $(B+C)/2$ for $NH_3{\cdot}H_2O$, $NH_3{\cdot}DOH$, and $ND_3{\cdot}D_2O$. The best fit occurred with R near 3 Å, θ_O near a hydrogen-bonded value with H_2O as the proton donor ($\theta_O = 52°$ in our coordinate system), and $\chi_O = 0$. An exact fit was not possible even though only three rotational constants were being fitted. The reason for this is that, as shown by Eq. (10), the $(B+C)/2$ values depend on χ_O through $\cos\chi_O$, which varies only slightly (6%) from unity within the range of $\pm 20°$ from zero. Zero-point vibrational effects are then large enough to prevent an exact fit. Since this preliminary fit showed clearly that the complex contained a linear N···H–O hydrogen bond ($\chi_O = 0°$, $\theta_O = 52°$) within the limits of the model, a second fit was done in which χ_O was fixed at zero and the distance R was allowed to differ depending on whether the isotopic species contained a hydrogen bond or a deuterium bond. Since $(B+C)/2$ depends primarily on R, this is the most likely source of the zero-point vibrational effects mentioned above, and such effects have been observed in other hydrogen bonded complexes.[14] Thus the three $(B+C)/2$ constants were fitted exactly by varying two different R values (N···H–O and N···D–O) and θ_O, with χ_O fixed at zero and θ_N taken from the eqQ data. The results are given in Table VI. The uncertainties in these results are from remaining zero-point vibrational effects, and are difficult to estimate. If the results are viewed as a vibrationally averaged structure, uncertainties of 5° in the angles and 0.002 Å for the R values are reasonable, with larger variations from the equilibrium structure likely, particularly for the O···N distances, which might vary by several hundredths of an Å from the equilibrium values.

As a check on the above results, $(B+C)/2$ for the fourth isotopic species can be calculated. Assuming it to be $NH_3{\cdot}HOD$, the geometry in Table VI gives $(B+C)/2$ of 5886 MHz, only 7 MHz higher than the experimental value. This is very good agreement, as a change of θ_O of less than 2° or a change in R of less than 0.002 Å would account for the difference. If this species is $NH_2D{\cdot}H_2O$, the rotational constants become dependent on χ_N and ϕ_N through the asymmetric ammonia. Variation of the latter coordinate ϕ_N through its entire range changes $(B+C)/2$ by less than 10 MHz, and thus it is not determined by this data. By varying χ_N with the other coordinates fixed at the values in Table VI, the observed $(B+C)/2$ is calculated for $\chi_N = 94°$, which puts the deuterium nearly perpendicular to the N···H_2O plane. If ϕ_N is varied, the χ_N value changes by less than 10° from the above result. Other reasonable interpretations of this data can be made. If the ammonia is undergoing nearly free internal rotation about its symmetry axis, it is more appropriate to average $(B+C)/2$ over χ_N. Again using the results in Table VI for the other coordinates, such an average gives 5870 MHz, close to the observed result. Another possibility is to average $(B+C)/2$ by assuming the ammonia is acting as a two-dimensional oscillator with an equilibrium value of $\theta_N = 0°$ and a root-mean-square amplitude of 23°, as suggested earlier. The averaging is carried out explicitly because $(B+C)/2$ for the species with an asymmetric ammonia will have a different dependence on θ_N than in Eq. (10) and fixing θ_N at 23° is no longer necessarily valid. For a range of χ_N values, the above procedure gives $(B+C)/2$ val-

TABLE VI. Structural data for $NH_3{\cdot}H_2O$.

R(N···H–O)/Å	2.983
R(N···D–O)/Å	2.979
θ'_N($NH_3{\cdot}H_2O$)/deg.	23.1 (2)
θ'_N($ND_3{\cdot}D_2O$)/deg.	20.4 (5)
θ_O/deg	56
χ_O/deg	~0
ω_s/cm^{-1}	168 (3)
k_s/mdyne/Å	0.145 (5)

ues from 5864–5872, again somewhat below the observed value, but within reasonable agreement. From these calculations, it is clear that the geometry in Table VI is consistent with the spectra observed for this fourth isotopic species. Because of the ambiguities pointed out above, it does not appear possible to make an isotopic assignment in this case and to use the data with certainty in the structure calculation. This latter point was not unexpected. Since both NH_3 and H_2O have similar masses, bond angles, and bond lengths, a linear, hydrogen-bonded structure will put a deuterium, on either group, at about the same distance from the principal axis of inertia of the complex. Since the inertia tensor depends strongly on this distance, but not on its sign, the ambiguity results.

The dipole moment results in Table III are also in agreement with the above picture of the $NH_3 \cdot H_2O$ geometry. With NH_3 and H_2O dipole moments of 1.472 D [15] and 1.855 D [16], respectively, a μ_a for the complex of 2.39 D is calculated. The experimental value is larger by 0.59 D, an enhancement which is in agreement with those for similar complexes, 0.46 D for $(H_2O)_2$ [17] and 0.60 D for $(HF)_2$.[18] The $\mu_\perp$ value is similarly expected to be 1.54 D, substantially larger than the observed values of 0.52 and 1.21 D for $NH_3 \cdot H_2O$ and $ND_3 \cdot D_2O$, respectively. This suggests that the water molecule is rotating around the N···H–O axis or that the H_2O hydrogens are switching roles, leading to tunneling splittings which would be expected to increase the energy separation between the $K = 0$ and $K = 1$ states. This would reduce the Stark effect caused by $\mu_\perp$ and reduce its value. Such tunneling splittings are very sensitive to reduced mass changes, and the observed $\mu_\perp$ for $ND_3 \cdot D_2O$ is in reasonably good agreement with the value expected from the structure.

The D_J value observed for $NH_3 \cdot H_2O$ can be used to calculate a psuedodiatomic stretching frequency and force constant from the expressions:

$$D_J = \frac{4[(B+C)/2]^3}{\nu_s^2}, \qquad k_s = 4\pi^2 \mu_r \nu_s^2. \tag{12}$$

ω_s and the associated force constant k_s are given in Table VI.

DISCUSSION

The ammonia–water complex is strikingly similar in its structure to the water dimer.[17] Both are linear hydrogen-bonded complexes with the proton acceptor at an angle suggesting tetrahedrally hybridized lone pairs of electrons pointing along the hydrogen bond. The heavy-atom separations for the two systems are within 0.01 Å of each other (2.98 Å). These distances are not equilibrium values and may be displaced by a few hundredths of an Angstrom from the equilibrium distances, but the agreement is, nonetheless, very close. The similarity extends to condensed phases as well. The O···O distance in ice is 2.84 Å,[19] identical to the N···O distance in the $2NH_3 \cdot H_2O$ crystal.[20] The decrease in these distances in the condensed phases presumably reflects cooperative effects—the charge redistribution on formation of one hydrogen bond enhances the formation of further hydrogen bonds.

The structures of hydrogen-bonded complexes can be rationalized by hybridized-lone pair, electron donor–acceptor models.[21–23] The similarity of the H_2O–H_2O and NH_3–H_2O systems is difficult to understand with this picture, however, at least with respect to the heavy atom separations. Ammonia is a better electron donor than water, and a stronger hydrogen bond with a shorter heavy atom separation might be expected for $NH_3 \cdot H_2O$ compared to $(H_2O)_2$. A shortening of this type is observed for $H_2O \cdot HF$[24] compared to $(HF)_2$ (or water dimer), with R (O···F) = 2.66 Å and R (F···F) = 2.79 Å. If significant charge transfer is involved in the hydrogen bond formation, the $NH_3 \cdot H_2O$ electric dipole moment might be expected to be more enhanced than for $(H_2O)_2$. Thus the $NH_3 \cdot H_2O$ enhancement is somewhat greater, but probably not significantly so, particularly given some uncertainty in the angular geometry of the complex. A 5° change in the angle of one of the water molecules would be sufficient to eliminate the difference in the enhancements. It is interesting to note that the enhancement for $H_2O \cdot HF$ is 0.96 D, substantially larger than for $(H_2O)_2$ or $(HF)_2$ (0.60 D).[24] Thus although the similarity in angular geometry for $NH_3 \cdot H_2O$ and $(H_2O)_2$ is readily accounted for by electron-pair, donor–acceptor models, the close parallels in the aspects mentioned above are not obvious in this picture and may be more easily explained with electrostatic models of hydrogen bonding.

There is no evidence to indicate that $NH_3 \cdot H_2O$ is an ionic complex $NH_4^+ \cdot OH^-$ or that the H_2O proton is partially transferred. The electric dipole moment and nitrogen quadrupole coupling should be particularly sensitive to even a partial proton transfer, but appear to be typical of NH_3 and H_2O complexes for which proton transfer is not indicated.[3,4,17] Some degree of ionic character or proton transfer has been suggested in matrix isolation studies of $NH_3 \cdot HCl$[25] and in *ab initio* calculations of methyl substituted $NR_3 \cdot HCl$ complexes.[26] However, this is not the case for $NH_3 \cdot H_2O$. It will be interesting to compare the $NH_3 \cdot H_2O$ result in this regard with $NH_3 \cdot H_2S$ since H_2S is a better acid than H_2O. Preliminary evidence suggests, however, that this molecule has a relatively long hydrogen bond with no indication of ionic character.[27]

Several *ab initio* calculations of the $NH_3 \cdot H_2O$ complex have been performed,[28–31] with good agreement with the geometry presented above. The best agreement with the heavy atom separation occurred for the 6-31G* basis[28] (3.05 Å) and the 4-31 G (0) basis[30] (2.95 Å). As is typically the case for hydrogen-bonded dimers, the dipole moments are substantially overestimated. For the two basis sets mentioned above, the dipole moment is calculated as 4.3 and 5.0 D, respectively. We calculated a total moment of 3.02(5) D from μ_a and $\mu_\perp$. Even given the large uncertainty in $\mu_\perp$, the *ab initio* values are clearly somewhat too high.

ACKNOWLEDGMENT

This work was supported by the Air Force Office of Scientific Research (F49620-83-C-0007).

[1]A. Werner, Ber. Dtsch. Chem. Ges. **36**, 147 (1903).
[2]T. S. Moore and T. F. Winmill, J. Chem. Soc. **101**, 1635 (1912).
[3]G. T. Fraser, K. R. Leopold, D. D. Nelson, Jr., A. Tung, and W. Klemperer, J. Chem. Phys. **80**, 3073 (1984).
[4]G. T. Fraser, K. R. Leopold, and W. Klemperer, J. Chem. Phys. **80**, 1423 (1984).
[5]G. T. Fraser, K. R. Leopold, and W. Klemperer, J. Chem. Phys. **81**, 2577 (1984).
[6]T. R. Dyke, Top. Curr. Chem. **120**, 85 (1984).
[7]D. Patel, D. Margolese, and T. R. Dyke, J. Chem. Phys. **70**, 2740 (1979).
[8]J. S. Muenter, J. Chem. Phys. **48**, 4544 (1968).
[9]N. F. Ramsey, *Molecular Beams* (Oxford University, London, 1963), Chap. III.
[10]A. E. Barton, D. J. B. Howlett, and B. J. Howard, Mol. Phys. **41**, 619 (1980).
[11]E. B. Wilson, Jr., J. C. Decius, and P. C. Cross, *Molecular Vibrations* (McGraw–Hill, New York, 1955).
[12]J. T. Hougen, J. Chem. Phys. **57**, 4207 (1971).
[13]R. Viswanathan and T. R. Dyke, J. Chem. Phys. **82**, 1674 (1985).
[14]Reference 6, Table III.
[15]M. D. Marshal and J. S. Muenter, J. Mol. Spectrosc. **85**, 322 (1981).
[16]T. R. Dyke and J. S. Muenter, J. Chem. Phys. **59**, 3125 (1973).
[17](a) T. R. Dyke, K. M. Mack, and J. S. Muenter, J. Chem. Phys. **66**, 498 (1977); (b) J. A. Odutola and T. R. Dyke, *ibid.* **72**, 5062 (1980).
[18]T. R. Dyke, B. J. Howard, and W. Klemperer, J. Chem. Phys. **56**, 2442 (1972).
[19]S. W. Peterson and H. A. Levy, Acta Crystallogr. **10**, 70 (1957).
[20]W. J. Siemons and D. H. Templeton, Acta Crystallogr. **7**, 194 (1954).
[21]K. C. Janda, J. M. Steed, S. E. Novick, and W. Klemperer, J. Chem. Phys. **67**, 5167 (1977).
[22]A. S. Georgiou, A. C. Legon, and D. J. Millen, Proc. R. Soc. London Ser. A **373**, 511 (1981).
[23]R. Viswanathan and T. R. Dyke, J. Chem. Phys. **77**, 1166 (1982).
[24]J. W. Bevan, Z. Kisiel, A. C. Legon, D. J. Millen, and S. C. Rogers, Proc. R. Soc. London Ser. A **372**, 441 (1980).
[25]B. S. Ault and G. C. Pimentel, J. Phys. Chem. **77**, 1649 (1973); B. S. Ault, E. Steinback, and G. C. Pimentel, *ibid.* **79**, 615 (1975).
[26]Z. Latajka, S. Sakai, K. Morokuma, and H. Ratajczak, Chem. Phys. Lett. **110**, 464 (1984).
[27]P. Herbine and T. R. Dyke (to be published).
[28]J. D. Dill, L. C. Allen, W. C. Topp, and J. A. Pople, J. Am. Chem. Soc. **97**, 7220 (1975).
[29]P. A. Kollman and L. C. Allen, J. Am. Chem. Soc. **93**, 4991 (1971).
[30]W. C. Topp and L. C. Allen, J. Am. Chem. Soc. **96**, 5291 (1974).
[31]W. A. Lathan, L. A. Curtiss, W. J. Hehre, J. B. Lisle, and J. A. Pople, Prog. Phys. Org. Chem. **11**, 175 (1974).